

Nonparametric reconstruction of dynamical dark energy via observational Hubble parameter data

Hao-Ran Yu,¹ Shuo Yuan,¹ and Tong-Jie Zhang^{1,*}

¹*Department of Astronomy, Beijing Normal University, Beijing 100875, China*

We study the power of current and future observational Hubble parameter data (OHD) on non-parametric estimations of the dark energy equation of state, $w(z)$. We propose a new method by conjunction of principal component analysis (PCA) and the criterion of goodness of fit (GoF) to reconstruct $w(z)$, ensuring the sensitivity and reliability of the extraction of features in EoS. We also give an new error model to simulate future OHD data, to forecast the power of future OHD. The result shows that current OHD, despite in less quantity, give not only a similar power of reconstruction of dark energy compared to the result given by type Ia supernovae, but also extend the constraint on $w(z)$ up to redshift $z \simeq 2$. Additionally, a reasonable forecast of future data in more quantity and better quality greatly enhances the reconstruction of dark energy.

PACS numbers: 98.80.Es 95.36.+x

I. INTRODUCTION

One of the main challenges of the modern physical cosmology is to study the nature of dark energy. Its evolution and dynamical properties are characterized by its equation of state (EoS). A cosmological constant is usually the simplest model to explain dark energy and its EoS remains constant $w(z) = -1$. Variations of the dark energy models, such as Quintessence, phantom, Quintoms etc., are also used to explain the dark energy. Studying dark energy in a parametrized way, such as CPL parametrization [1, 2] may induce misleading results due to our prior assumptions of function forms of EoS, then we may direct reconstruct EoS non-parametrically [3]. This has been achieved by astronomical data, such as luminosity distances d_L of type Ia supernovae (Ia SN) [4, 5]. Although we have plenty of Ia SN data, it requires the second derivative of d_L respect to redshift z , and a complicated form of reconstruction equation. While, observational Hubble parameter data (OHD) reconstruct $w(z)$ via a simpler way (Eq.(2)) and require only the first derivative of $H(z)$, so it is more stable and less sensitive to the error of the data. From the last decade, OHD are proved to be very powerful in the constraint of cosmological parameters [6], it responses the cosmic expansion history directly and can be measured by various methods, e.g. cosmic chronometers [7], baryonic acoustic oscillation (BAO) peaks [8], and even other proposed Sandage-Loeb (SL) probes and standard siren by gravitational waves. On the way of obtaining more data from observations, to simulate sets of future OHD appropriately is also instructive at the current stage in exploring the quality of EoS reconstruction in the near future. To do this, we need an error model giving the redshift distribution, the offsets from the theoretical value, and the sizes of their error bars, such as in [9]. Here we construct a new and more accurate error model for next generation surveys, carefully estimating potential power of observation in different methods.

For either observational or our simulated data, reconstructing $H(z)$ and $w(z)$ from data confronts the trading between extracting more features and being polluted by the errors (over-fitting). Principle component analysis (PCA) is usually used to exclude error-induced oscillations in the reconstructing processes [4], and

information criteria [10] are often used for choosing models [5]. We also find that the goodness of fit (GoF) is a effective probe of over-fitting. The conjunction of PCA and GoF works naturally to deal with this tradeoff.

The rest of the paper is organized as follows. We present our reconstruction method in Sec.II, and briefly illustrate the current OHD and forecast future OHD in Sec.III. We show the results by our method in Sec.IV and conclude in Sec.V.

II. METHOD

A. Reconstruction

The expansion of the universe is affected by the densities of the components and the state of dark energy:

$$H(z)^2 = H_0^2[\Omega_M(1+z)^3 + \Omega_K(1+z)^2 + \Omega_\Lambda g(z)], \quad (1)$$

where Ω_M , Ω_K , Ω_Λ are the current energy density in matter, curvature and dark energy: $\Omega_M + \Omega_K + \Omega_\Lambda = 1$, and $g(z) = \exp\left[3 \int_0^z (1+w(z'))/(1+z')dz'\right]$. Expressing $w(z)$ in terms of $H(z)$ and $H'(z) \equiv dH/dz$ and we get the reconstruction equation:

$$w(z) = \frac{3H^2 - 2(1+z)HH' - \Omega_K H_0^2(1+z)^2}{3H_0^2(1+z)^2[\Omega_M(1+z) + \Omega_K] - 3H^2}. \quad (2)$$

Given a set of $H(z)$ data \mathbf{y} , we fit them by a smooth analytical function then use it and its first derivative to reconstruct $w(z)$ by Eq.(2). Assume the data $\mathbf{y} = (y_1, y_2, \dots, y_n)^T$ with covariance matrix \mathbf{C} . By choosing a set of N ($N < n$) primary basis functions such as polynomials, rational functions or wavelets: $\mathbf{X} = (\mathbf{x}_1^T, \mathbf{x}_2^T, \dots, \mathbf{x}_N^T)$, where \mathbf{x}_i is a row vector representing the i th basis, we fit \mathbf{y} by linear least squares. Simply minimize the weighted squared residual $\mathcal{R} = (\mathbf{y} - \mathbf{X}\boldsymbol{\beta})^T \mathbf{C}^{-1}(\mathbf{y} - \mathbf{X}\boldsymbol{\beta})$ by solving $\partial \mathcal{R} / \partial \boldsymbol{\beta} = \mathbf{0}$, and we get the coefficient vector

$$\boldsymbol{\beta} = (\mathbf{X}^T \mathbf{C}^{-1} \mathbf{X})^{-1} \mathbf{X}^T \mathbf{C}^{-1} \mathbf{y}. \quad (3)$$

By enough realizations from the error model, we diagonalize the inverse covariance matrix of $\boldsymbol{\beta}$ by finding its N eigenvalue and eigenvectors: $\mathbf{F} = \text{Cov}^{-1}(\boldsymbol{\beta}) = \mathbf{E} \boldsymbol{\Lambda} \mathbf{E}^T$, where $\mathbf{E} = (\mathbf{e}_1^T, \mathbf{e}_2^T, \dots, \mathbf{e}_N^T)$ rearranges the N primary basis functions to N new orthogonal

* tjzhang@bnu.edu.cn

eigenbasis $U = XE$ with the corresponding eigenvalues $\text{diag}(\Lambda) = (\lambda_1, \lambda_2, \dots, \lambda_N)^T$. The first M ($M \leq N$) eigenmodes $U_M = XE_M$, where $E_M = (e_1^T, e_2^T, \dots, e_M^T)$, the principal components of the data, are usually of our interest, reflecting the main features of data. Conversely, the rest components are induced by the random offsets in the data and may induce overfittings. After the rearrangement, we solve Eq.(3) again and get new coefficients for the new basis:

$$\beta_M = (U_M^T C^{-1} U_M)^{-1} U_M^T C^{-1} y. \quad (4)$$

Because we have enough realizations to estimate $\text{Cov}(\beta)$, and any single new realization or observational data, having similar configurations, their true features can still be extracted and the nuisance features are excluded. With the reliable smooth $H(z)$, getting $w(z)$ is straightforward from Eq.(2) and its errors can be estimated from realizations.

B. An optimal error model

Usually simulated offsets and errors are regarded as Gaussian distributed [9]. More generally, the error, a random variable σ , is determined by several factors $\mathbf{t} = (t_1, t_2, \dots, t_k)^T$, where these factors are assumed to be Gaussian distributed with covariance Σ_t . These factors are different sources of errors that jointly contribute to σ by a quadratic form $\sigma^2 = \mathbf{t}^T \mathbf{D} \mathbf{t}$, and the matrix \mathbf{D} denotes the relation between factor and the final error, up to the second order accuracy. In such case, σ has a Nakagami m -distribution $f_m(x; m, \Omega)$ (a scaling transform of generalized- χ -distribution with parameters Σ_t and \mathbf{D}) [11], and has a complicated form. We can never estimate the full contribution of these factors (weather, telescope, device, recording during observation, as long as data reduction and systematic errors etc.), however, we simplify the problem by assuming $t_i \sim \mathcal{N}(0, 1)$, $\Sigma_t = \mathbf{D} = \mathbf{I}$: they are independent, having same importance, and contribute to σ^2 additively. In this case, $\sigma \sim \chi_k$. More realistically, there are few dominant factors, of much greater importance ($\Sigma_t \neq \mathbf{I}$), jointly contribute to the final error. This effectively cause a reduction in the degree of freedom, $k \rightarrow k'$ ($k' < k$) and a scaling transform ($\chi_{k'} \rightarrow A\chi_{k'}$). Practically, neglecting the mathematics details, we find that the m -distribution $f_m(x; m, \Omega)$ ($m = k'/2$, $\Omega = A^2/k'$) well matches the relative error σ_H/H 's distribution and does not depend on redshift z .

The redshift distribution is generated according to the configuration of each method of measurement. For large enough sample, we find that uniform distributed or evenly spaced samples are good approximations. For errors and offsets, we assume the data points are independent, so the relative error is successively generated from the correspond distribution $\sigma/H_\star(z) \sim f_i$ where f_i is the relative error distribution for the i th kind measurement. This means that, we are ready for a measurement, without knowing the true value $y_\star = H_\star(z)$, but the quality (error bar) is predetermined. For $\langle f_i \rangle \ll 1$, the resulting measurement should have the distribution $y \sim \mathcal{N}(y_\star, \sigma)$, and it gives the simulated data.

C. Goodness of fit

The remaining problem is how to choose the number of primary basis functions N and the number of reserved principal components M appropriately. The choice of (N, M) directly relates to the upper limit of the ability of how complex we can detect the features of the underlying model. If we suppose that the fitted model is just the underlying model, the offset $y - y_\star$, having the distribution of $\mathcal{N}(0, \sigma)$, contributes to the residual R_\star by $(\mathcal{N}(0, 1))^2$ for each independent data point, and R_\star has χ^2 -distribution $R_\star \sim \chi_n^2$. Thus

$$\langle \text{GoF}_\star \rangle \equiv \left\langle \frac{R_\star}{n} \right\rangle = \left\langle \frac{(y - y_\star)^T C^{-1} (y - y_\star)}{n} \right\rangle = 1. \quad (5)$$

Here we use \star to denote that the fitted model is replaced by the underlying model, and also define R_\star/n as the ‘‘goodness of ‘fit’’ for underlying model GoF_\star . Going back to the resulting fitted model, define the GoF in our circumstance as¹

$$\text{GoF} \equiv \frac{\mathcal{R}_M}{n-1}, \quad (6)$$

where \mathcal{R}_M is the least square \mathcal{R}_{\min} given by the first M principal components U_M :

$$\mathcal{R}_M = (y - U_M \beta_M)^T C^{-1} (y - U_M \beta_M). \quad (7)$$

Statistically $\langle \text{GoF} \rangle$ should also be unity. If less than, it indicates the overfitting of offsets due to the measurement error. Conversely, GoF greater than one for a great amount means that we not yet capture the full features of data, i.e. the model is too simple to fit all the features of data. We use GoF as the indicator to determine the complexity of our fitted model to avoid the above two conditions. Here, the complexity of fitted model is less or equal than the true underlying model because errors and offsets lower the detectability of the underlying model. Although the underlying true model, no matter its complexity, always let its generated data to have $\text{GoF}_\star \simeq 1$, the same configuration in complexity (N and M) leads to illness in fitting low quality data, because the errors and offsets are more dominant than the true features and thus be amplified and any subtler features are covered. As a result, the reconstructed model is no longer the underlying model and usually has much smaller GoF .

For given large enough N , fully usage of all eigenmodes ($M = N$) leads to the overfitting, and we degrade the complexity of model by reduce M consecutively while examine $\langle \text{GoF} \rangle$ over realizations, until we find the last M to have $\langle \text{GoF} \rangle > 1$ – it is still save to use this grade of complexity. Insufficient number of primary basis functions N causes two consecutive M 's to have a

¹ Note that, although it is usually to scale R_M by the degree of freedom $\nu = n - M - 1$, here we instead use $n - 1$ to scale R_M for estimated underlying model from n data samples. Because various choice of primary basis functions and inertial complexity of underlying model lead to different numbers of parameters needed. Even, given a fixed underlying model, resulting N and M depend on X . Thus the expression of GoF should not be scaled by anything in terms of N nor M in this circumstance.

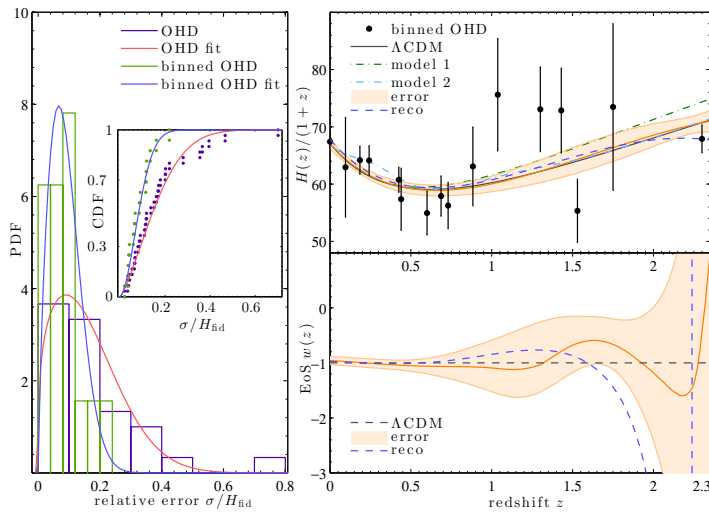


FIG. 1. (left:) Relative error distribution for OHD. The purple and green histograms show the relative errors of unbinned 28 OHD and binned 15 OHD, and the red and blue curves are their best fits by a m -distribution. Their counterpart CDF and fitted CDF are shown in the inset. (right:) Binned OHD and their reconstructions on $H(z)$ (top) and $w(z)$ (bottom). The shaded orange areas show the 1σ error regions if we assume a Λ CDM model. Dashed blue lines are the results from binned OHD.

great difference in $\langle \text{GoF} \rangle$ – skipping the range of appropriate fitting ($\langle \text{GoF} \rangle \simeq 1$), as the eigenmodes are poorly determined from limited number of primary functions, or the primary functions X are chosen improperly. In these cases we should either increase N or choose more suitable X .

Generally, there is not an optimal choice of primary function basis X as the possible underlying $H(z)$ is kaleidoscopic. Also, the underlying complexity of $w(z)$, thus $H(z)$ is also plumbless without the knowledge of essence of dark energy. However, we can still choose some popular, reasonable models to see how different X 's have effect on the fitting. Usually polynomials are more effective than other rational functions for not-too-complex models, and they form stable eigenmodes that are invariant for different values of N and various underlying $H(z)$, even if the underlying $H(z)$ is very oscillatory.

III. AVAILABLE AND FUTURE HUBBLE PARAMETER DATA

Current OHD are obtained primarily by the method of cosmic chronometer [12–15]. Other methods to extract $H(z)$ are by the observations of BAO peaks [8, 16], Ly- α forest of LRGs [17]. The last of which extended the current OHD deep to $z = 2.3$.

Assuming the independency of 28 measurements, to calculate the residual between the data and a theoretical Λ CDM model gives $\text{GoF}_\star = 0.62$. It indicates that the assumption is not accurate, however, we do not have a good estimation of the off-diagonal elements of the OHD's covariance matrix. To weigh the power of current OHD and compare with simulations, we rebin the data from LRGs that are with close redshifts, and get finally 15 measurements of OHD with smaller error bars (see figure 1). Now the $\text{GoF}_\star = 1.02$, which is close to independent measure-

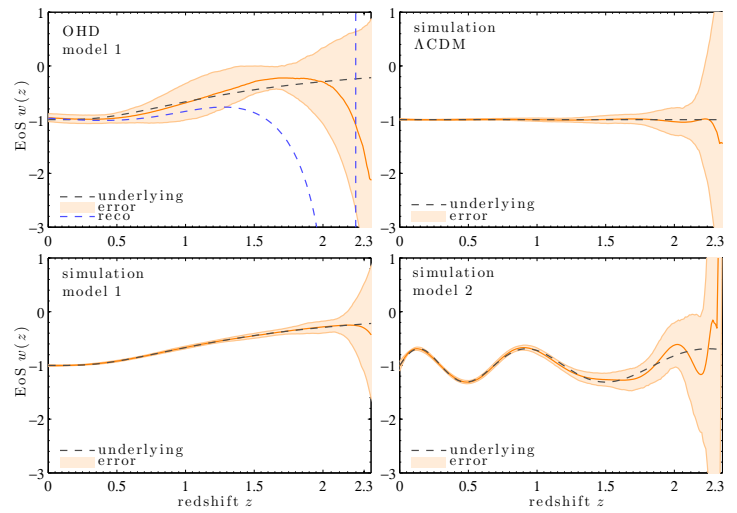


FIG. 2. (top-left:) Reconstruction of $w(z)$ by OHD's redshift and error configurations, but assuming model-1. Also shown in blue dashed line is the reconstruction of OHD set, which is obviously inconsistent with model-1. The rest three panels show the reconstruction of $w(z)$ from simulated future data, with the underlying model being Λ CDM, model-1 and model-2.

ments. Although this is only a rough estimation, it is still more accurate than the 28 data points with no knowledge of their covariance. The binned and unbinned error distributions for OHD from well match the shape of m -distribution (see the left panel of Fig.1). We also assume the relative error of future data to have such distribution.

There are several ways to enhance the quality of OHD, and of which deeper-redshift, more-complete-sky-coverage LRG survey and spectroscopic observations of those identified LRGs give remarkable improvement on the two methods on LRG. For example, the 2SLAQ² has provided a LRG catalogue with the redshift range from 0.3 to 0.9 with 180 deg² coverage of the sky. Considering a future LRG survey with more than half sky coverage with redshift range $z \sim 2.3$, it may give several millions of LRGs and effectively enlarges the number of OHD data points or lowers their errors. By an LRG sample binning strategy [12], up to 100 OHD measurements can be extracted with 20% of present error level.

Other methods are also potential: [16] give three OHD by processing the WiggleZ³ survey, fitting BAO peak parameter and the 2D power spectrum at three redshift slices. The raw WiggleZ samples are 158741 galaxies in the range $z = (0.2, 1.0)$ with 800 deg² coverage of the sky. We can also forecast a more-than-half-sky survey like WiggleZ, which offers up to five million targets and thus lowers the error level to several percent of present level. The more ambitious experiment for Sandage-Loeb signal(SLS), proposed by [18] and [19], may further deepen the redshift range of OHD. It measures the quasar Ly- α forest in a separation of few decades by the extremely large telescope like the European

² <http://www.2slaq.info/>

³ <http://wigglez.swin.edu.au/site/>

Extremely Large Telescope (E-ELT)⁴. The upcoming CODEX (COsmic Dynamics and EXo-earth experiment)⁵ is based on the E-ELT and offers a measurement of SL signal. If succeed, it can help us to explore the redshift from 2 to 5 covering the “redshift desert” and give useful data for the expanding history of the universe [20]. The CODEX group provided a full design of observing the SL signal and the prediction of the statistical error of SLS [21]. We use the SL signal, with an error estimation by [22] (15 years observational interval is assumed), as an optional simulated data to study its impact on the result.

IV. RESULTS

We set cosmological parameters Ω_M , Ω_K , Ω_Λ and H_0 as in the latest Planck data release [23]. For the diagnostic EoS models, we choose Λ CDM with $w_\Lambda(z) = -1$ and other two arbitrary models $w_1(z) = -1/2 + \text{erf}(\ln(2z/e))$ and $w_2(z) = -1 - 0.31 \sin(12 \ln(1/(1+z)))$, where model-1 w_1 smoothly varies from -1 to 0 as z increases, while model-2 w_2 is very oscillatory. The theoretical $H(z)$ curves based on these two models are shown in dash-dotted lines in the top-right panel of Fig.1. We also show the dashed blue line, representing the best-fit analytical $H(z)$ curve by using 15 binned OHD. Its reconstruction of $w(z)$ is shown in the bottom-right panel of Fig.1. We do not show errors for these two dashed blue lines – usually Monte-Carlo realizations are run on each data point: $y_{MC} \sim \mathcal{N}(y, \sigma)$ to get the statistical properties. However, recall that $y \sim \mathcal{N}(y_*, \sigma)$, so $y_{MC} \sim \mathcal{N}(y_*, \sqrt{2}\sigma)$: its error is amplified, and also we have only one realization – real observation, y_{MC} is biased by y , due to the cosmic variance. By such reason we can only get an error estimation based on a supposed underlying model, e.g. Λ CDM – assuming y is just one realization of y_* , and we calculate the statistics from other realizations from y_* : $y_{MC} \sim \mathcal{N}(y_*, \sigma)$, and see if the reconstruction from the real data is within the error region of y_{MC} . We use our error model to simulate data and do this Monte-Carlo realization. Here we use only cosmic chronometer data, with 100 independent measurements, 20% of present error level, evenly distributed on $0 < z < 2.3$. The results are shown with expectations (orange lines) and 1σ their error regions (translucent orange areas) in Fig.1. For $H(z)$, it reasonably covers the $H(z)$ by underlying Λ CDM. $w(z)$ is confident when $z \lesssim 1.5$, while beyond this range the reconstruction is biased due to the scarceness of data, and when $z \approx 2$ it is even hopeless because H' is badly determined. Comparing the the result (blue dashed line) with the error region, we still see a obvious $\sim 1.5\sigma$ deviation from Λ CDM at $1.6 \lesssim z \lesssim 2$ and it does not correlate with the bias of the central

line of the error region. This is caused by the Hubble parameter datum at $z = 2.3$, with a small error bar, and which is deviated from Λ CDM. This feature is also similar to the result by Ia SNe [5]. Our forecast of future data is proved to be able to verify or refute this deviation. The top-left panel of Fig.2 shows another Monte-Carlo simulation, with Λ CDM replaced by model-1, and we can see that the reconstructed line by OHD is obviously excluded by this model. The rest three panels in Fig.2 show the results by simulated future OHD with underlying models being Λ CDM, model-1 and model-2 respectively. Note that, for varying quality of data and underlying model complexity, (N, M) are automatically adjusted, and are no longer suitable for current OHD, so we do not include current reconstructions. We can see that future OHD are able to reconstruct $w(z)$ very accurately, even for very oscillatory models.

V. DISCUSSION AND CONCLUSION

We propose a new method by combining PCA and GoF to reconstruct dark energy EoS $w(z)$ by OHD. We compare the results from current available and future OHD, where we use a more accurate error model to simulate future OHD. We discover a feature of deviation from Λ CDM at $z > 1.5$ and Ia SN data give similar results [5]. Future data simulations greatly enhance the result (Fig.2), and are able to confirm or deny this deviation. In the analysis we used only cosmic chronometer data. We also use simulations with the data from other sources (BAO, SL signals), and the result does not improve much. Because the quantity of three BAO data and five SL data dominates only a small fraction of total 100 simulated data. However, with small number, say 20, of cosmic chronometer data, adding several SL signal data lowers the error of reconstruction at $z \approx 2$, but beyond this redshift the result is still not confident. The reason is that, adding a few high-redshift data helps to determine H' better at $z \approx 2$ but is still unable to well determine H' at $2 \lesssim z \lesssim 5$. In such case we may use a derivative prior in Eq.(3) or use a Gaussian process [24] to help to determine H' .

ACKNOWLEDGEMENTS

HRY thanks Ue-Li Pen for helpful discussions. This work was supported by the National Science Foundation of China (Grants No. 11173006), the Ministry of Science and Technology National Basic Science program (project 973) under grant No. 2012CB821804, and the Fundamental Research Funds for the Central Universities.

[1] M. Chevallier and D. Polarski, International Journal of Modern Physics D **10**, 213 (2001), arXiv:gr-qc/0009008.

⁴ <http://www.eso.org/public/teles-instr/e-elt.html>

⁵ <http://www.iac.es/proyecto/codex/>

[2] E. V. Linder, Physical Review Letters **90**, 091301 (2003).

[3] G.-B. Zhao, R. G. Crittenden, L. Pogosian, and X. Zhang, Physical Review Letters **109**, 171301 (2012), 1207.3804.

[4] D. Huterer and G. Starkman, Physical Review Letters **90**, 031301 (2003), arXiv:astro-ph/0207517.

[5] C. Clarkson and C. Zunckel, Physical Review Letters **104**, 211301 (2010), 1002.5004.

- [6] Z.-L. Yi and T.-J. Zhang, *Modern Physics Letters A* **22**, 41 (2007), arXiv:astro-ph/0605596.
- [7] R. Jimenez and A. Loeb, *Astrophys. J.* **573**, 37 (2002), arXiv:astro-ph/0106145.
- [8] E. Gaztañaga, A. Cabré, and L. Hui, *Mon. Not. R. Astron. Soc.* **399**, 1663 (2009), 0807.3551.
- [9] C. Ma and T.-J. Zhang, *Astrophys. J.* **730**, 74 (2011), 1007.3787.
- [10] A. R. Liddle, *Mon. Not. R. Astron. Soc.* **377**, L74 (2007), arXiv:astro-ph/0701113.
- [11] J. Sheil and I. O’Muircheartaigh, *Journal of the Royal Statistical Society. Series C* **26**, 92 (1977).
- [12] J. Simon, L. Verde, and R. Jimenez, *Phys. Rev. D* **71**, 123001 (2005), arXiv:astro-ph/0412269.
- [13] D. Stern, R. Jimenez, L. Verde, S. A. Stanford, and M. Kamionkowski, *Astrophys. J. Suppl. Ser.* **188**, 280 (2010), 0907.3152.
- [14] M. Moresco *et al.*, *J. Cosmology Astropart. Phys.* **8**, 6 (2012), 1201.3609.
- [15] C. Zhang, H. Zhang, S. Yuan, T.-J. Zhang, and Y.-C. Sun, *ArXiv e-prints* (2012), 1207.4541.
- [16] C. Blake *et al.*, *Mon. Not. R. Astron. Soc.* **425**, 405 (2012), 1204.3674.
- [17] N. G. Busca *et al.*, *Astron. Astrophys.* **552**, A96 (2013), 1211.2616.
- [18] A. Sandage, *Astrophys. J.* **136**, 319 (1962).
- [19] A. Loeb, *Astrophys. J. Lett.* **499**, L111 (1998), arXiv:astro-ph/9802122.
- [20] P.-S. Corasaniti, D. Huterer, and A. Melchiorri, *Phys. Rev. D* **75**, 062001 (2007), arXiv:astro-ph/0701433.
- [21] J. Liske *et al.*, *Mon. Not. R. Astron. Soc.* **386**, 1192 (2008), 0802.1532.
- [22] M. Martinelli, S. Pandolfi, C. J. A. P. Martins, and P. E. Vielzeuf, *Phys. Rev. D* **86**, 123001 (2012), 1210.7166.
- [23] Planck Collaboration, *ArXiv e-prints* (2013), 1303.5076.
- [24] M. Seikel, S. Yahya, R. Maartens, and C. Clarkson, *Phys. Rev. D* **86**, 083001 (2012), 1205.3431.